Natural acidic deep eutectic solvent to obtain cellulose nanocrystals using the design of experience approach

L. Douard, J. Bras, T. Encinas, M.N. Belgacem

Natural acidic deep eutectic solvent to obtain cellulose nanocrystals using the design of experience approach.

Douard L.[1], Bras J.[1,2], Encinas T.[3], Belgacem N.[1,4•]

1. Univ. Grenoble Alpes, CNRS, Grenoble INP*, LGP2, F-38000 Grenoble, France
2. Nestle Research Center, CH-1000 Lausanne, Switzerland
3. Univ. Grenoble Alpes, Grenoble INP*, CMTC, F-38000 Grenoble, France
4. Institut Universitaire de France (IUF), F-75000 Paris, France
*Intitute of Engineering Univ. Grenoble Alpes
•Contact: mohamed-naceur.belgacem@grenoble-inp.fr

Abstract

In this study, a new approach to optimize the cellulose nanocrystals (CNCs) extraction using acidic natural deep eutectic solvents (NADES) was introduced using, for the first time, design of experiment method. Choline chloride:oxalic acid dihydrate with a molar ratio of 1:1 was used to extract CNCs. Then, three most important parameters were varied to design the experiment: (i) cotton fibre concentrations, (ii) temperature and (iii) treatment time. Two outcomes were studied: the CNC yield and the crystallinity. The mathematical model for crystallinity perfectly described the experiments, while the model for CNC yield provided only a tendency. For a reaction time of 6 h at 95°C with a fibre concentration of 2%, the expected optimum CNC yield was approximately 35.5 ± 2.7% with a crystallinity index of 80 ± 1%. The obtained experimental results confirmed the models with 43.6 ± 1.9% and 81 ± 1% for the CNC yield and the crystallinity index, respectively. This study shows that it is possible to predict the CNC yield CNC and their crystallinity thanks to predictive mathematical models, which gives a great advantage to consider in the near future a scale up of the extraction of cellulose nanocrystals using this original family of green solvents.

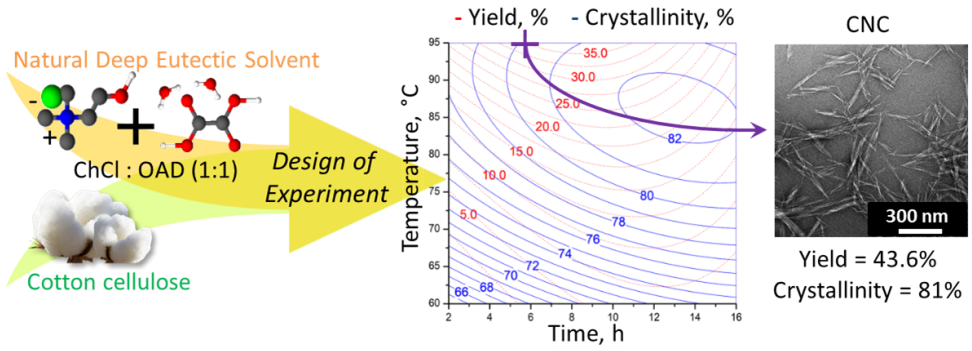

Keywords: Cellulose nanocrystal – Natural Deep Eutectic Solvents – Design of Experiment – High crystallinity – Treatment optimisation

Highlights

- Cellulose nanocrystals are successfully extracted using a natural deep eutectic solvent.

- The influence of the treatment time, temperature, and initial fiber concentration during the CNC extraction was studied and thoroughly described using mathematical models.
- 16 different parameter combinations are employed to build and to check the validity of these two mathematical models.
- Cellulose nanocrystals having optimal yield and crystallinity of 44.9% and 81%, respectively, were obtained.

1. Introduction

In 1947, Nickerson and Habrle were among the first to reveal the existence of a crystalline part on cellulosic fibres and isolate it using an acid hydrolysis process in 1947 (Nickerson and Habrle, 1947). Since the 1960s, cellulose nanocrystals (CNCs) have been extracted *via* sulfuric acid hydrolysis of the cellulose amorphous parts. CNCs have many characteristics that make them suitable for the development of innovative materials for various applications, e.g., the abundance of biosourced starting materials, their low density (1.6 g/cm^3), and their high stiffness and specific surface area. Moreover, due to the presence of hydroxyl groups on their surface, CNCs are hydrophilic and reactive for post-modification to provide new functionalities. Biobased CNC nanoparticles are now commercially available (Reid, Villalobos, and Cranston, 2017), and they show promising results in various applications, such as biocomposites (Mariano, Kissi, and Dufresne, 2014), hydrogels (Du *et al.*, 2019), rheological modifiers (Gicquel *et al.*, 2019), tissue engineering and health care applications (Domingues, Gomes, and Reis 2014; Shankaran, 2018) and coatings (Mascheroni *et al.*, 2016).
CNCs are rod-shaped particles with the following nanometric dimensions: their lengths are approximately 100 to 500 nm depending on the cellulose source (Bras et al. 2011) and their diameters are between 5 and 20 nm (Ramires and Dufresne, 2011; Isogai, 2020).
CNCs can be extracted by hydrolysing glyosidic bound of the amorphous part of cellulosic fibres. Sulfuric acid (H_2SO_4) is the most common acid used to obtain CNCs; indeed, this common procedure can be applied to any cellulose source with small adaptations, as sketched in scheme 1.

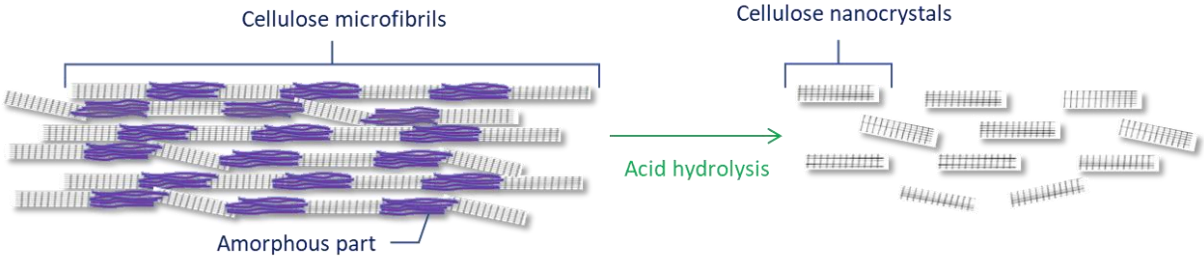

Scheme 1: Schematic representation of acid hydrolysis of cellulose fibre

Recently published reviews identify all the different conditions that can be used to extract cellulose nanocrystals with this “conventional hydrolysis”. (Dufresne 2017; Haldar and Purkait 2020). However, it was proved that the CNC yield, and their properties strongly depend of the cellulose sources and treatment conditions (time and temperature of treatment, and initial acid concentration). Thus, for example, Flauzino Neto *et al.* extracted cellulose nanocrystal from soy hull using H_2SO_4 64% treatment, and

showed that prolonging the reaction by 10 min decrease the CNC length and reduce their crystallinity (Flauzino Neto *et al.,* 2013).

However, other methods enable CNC extraction from biomass. For example, other types of acids have been used, such as hydrochloric acid (Araki *et al.* 1999) or organic acid (Filson and Dawsonandoh, 2009). Subcritical water (Novo *et al.* 2015) or ionic liquid (Man *et al*. 2011) have also been used for cellulose nanocrystal extraction. More recently, a new solution was proposed that consists of using acidic deep eutectic solvents as reactive media (Zdanowicz, Wilpiszewska, and Spychaj 2018).

Deep eutectic solvents (DESs) are a new class of organic solvents that were introduced for the first time in 2003 by Abbott *et al*., who found that the eutectic mixture formed by choline chloride and urea with a molar ratio of 1:2 exhibited a freezing point of 12°C, which is considerably lower than that of either of the constituents (choline chloride = 302°C and urea = 133°C) (Abbott *et al*., 2003). DESs are in a state of molten salt and ionic liquid solvent, but compared to other solvents, they are easier to use and less toxic and are composed of a Lewis or Brönsted acid and a base with a specific ratio. According to the nature of these two constituents, DES can be classified into four types (Smith, Abbott, and Ryder, 2014).

In the case of DES type III, the two constituents are a quaternary ammonium salt and a hydrogen bond donor; the association of these compounds results in a eutectic mixture *via* hydrogen bonding interactions between the hydrogen bond acceptor and the hydrogen bond donor. The melting temperature of the mixture, far below that of its individual constituents, can be explained by the fact that the strong hydrogen bonds between the different compounds prevent the crystallization of each product (Francisco, van den Bruinhorst, and Kroon, 2013). Moreover, if the DES is formulated with natural compounds, the obtained mixture is referred to as natural deep eutectic solvent (NADES), which can be considered a green solvent due to its nonvolatility, low toxicity, and potential renewability, recyclability and biodegradability (Paiva *et al.* 2014; Vanda *et al*., 2018).

DES and NADES are easy to obtain and can be helpful in organic chemistry ; indeed, they can replace some toxic organic solvents in a large number of application fields. In a recent review, Zdanowicz *et al*. summarized the possible application range of DES and NADES for polysaccharide processing (Zdanowicz, Wilpiszewska, and Spychaj, 2018). One of these applications used of Type III NADES as an acidic hydrolytic solvent to obtain CNCs. NADESs exhibit lower vapour pressures than aqueous solutions and thus can be considered safer than aqueous solutions. Moreover, recent studies have claimed the possibility of reusing DES five times without a decrease in their efficiency (Li *et al*. 2018; Liu *et al*., 2017). These two advantages indicate that NADES should be more deeply studied as a new method of cellulose nanocrystal production.

Many combinations of hydrogen bond donors and acceptors using different ratios can be used to obtain acidic deep eutectic solvents that can hydrolyse the amorphous parts of cellulose (Sirviö, Visanko, and Liimatainen, 2016; Ibrahim, Abdullah, and Sam, 2018; Sirviö 2019). However, the most studied NADES was used for the first time by Sirviö et al. in 2016 (Sirviö, Visanko, and Liimatainen, 2016). The researchers managed to extract individual cellulose nanocrystals using a choline chloride:oxalic acid dihydrate (ChCl:OAD 1:1) treatment from dissolving pulp. They used two different temperatures (T=100 or 120°C) and a reaction time of 2 hours. After this pre-treatment, NADES was removed using distilled water, and the suspension was disintegrated mechanically using a microfluidizer. The CNCs produced at 120°C showed a high aspect ratio with a length of approximately 353 ± 16 nm and a diameter of 9.9 ± 0.7 nm. Since this first study,

different studies using this NADES in different ratios, various experimental conditions, and different cellulose sources have been conducted to extracted CNCs. In 2017, Laitinen *et al*. showed that only 30 minutes of treatment at 100°C is enough to extract CNC from bleached birch Kraft pulp using ChCl:OAD 1:1 as the pre-treatment. The nanocrystals obtained are non-charged and can be used as oil-water Pickering stabilizers (Laitinen *et al*., 2017). However, a faster way to produce CNCs using this solvent is to assist the pre-treatment by microwave application. Using this technique, Liu *et al*. obtained a CNC suspension in only 3 minutes of reaction (Liu *et al*., 2017). More recently, Ling *et al*. studied the effect of ChCl:OAD treatment on the cellulose nanocrystal structure. They compared three ChCl:OAD molar ratios of 1:1, 1:2, and 1:3 at two temperatures of 80°C and 100°C. In all cases, they managed to obtain cellulose nanocrystals, but lower crystallinity and lamellar structures were observed for CNCs with a lower acid content treatment. The CNCs obtained with a higher acid ratio (ChCl:OAD 1:3) were more dispersed and exhibited a higher aspect ratio (Ling *et al.,* 2019). Inspired by the conventional acid hydrolysis treatment with H_2SO_4, Yang *et al*. proposed the use of a catalyst ($FeCl_3 \cdot 6H_2O$) during DES treatment. They varied the temperature of the treatment and the molar ratio of choline chloride, oxalic acid dihydrate, and catalyst and found that the optimum conditions for the treatment were 80°C and 6 h of treatment in ChCl:OAD:$FeCl_3 \cdot 6H_2O$ DES at a molar ratio of 1:4.43:0.1 *(Yang et al*., 2019).

All these studies have been conducted recently and have not provided clear information on the CNC yields. The possibilities to generate new acidic natural deep eutectic solvents are almost infinite; indeed, simply changing the molar ratio between the constituents of the solvent would result in a new solvent with new properties. The same is true if another acid is used as the hydrogen bond donor. Therefore, the aim of the present study is to examine the role of time and reaction temperature in the production of cellulose nanocrystals. Our hypothesis is that there is an optimum of parameters for obtaining higher yield of cellulose nanocrystals via DES treatment.

In this work, a design of experiment (DOE) approach is used to follow the yield of cellulose nanocrystals and their crystallinity with the commonly used natural deep eutectic solvent ChCl:OAD at a molar ratio of 1:1 by means of varying 3 parameters: (i) the temperature (60-95°C), (ii) the reaction time (2–16 h) and (iii) the cotton fibre cellulose concentration (1-2%). The DOE method allows process optimization by performing a minimum number of experiments while varying the 3 parameters at the same time. We first established a mathematical model to determine the optimal conditions of acid hydrolysis to obtain the highest yield, and then, we tried to predict the CNC crystallinity. Once the domain of the treatment conditions was perfectly described, it was possible to choose the proper combination of parameters to obtain nanocrystals with the desired yield and crystallinity.

2. Materials and methods

2.1. Materials

Dry sheets of commercially available of bleached and mechanically treated cotton fibre obtained from the paper industry were used as cellulosic material (CELSUR, CS 21 DHS). Oxalic acid dihydrate (≥ 99%) and choline chloride (≥ 98%) were obtained from Sigma-Aldrich, and sodium chloride (≥ 99%) was obtained from Roth. Deionized water was used throughout the experiment.

2.2. NADES treatment

The 1:1 molar ratio of acidic deep eutectic solvent was produced by stirring 63.0 grams of oxalic acid dihydrate and 69.8 grams of choline chloride continuously for 30 minutes at 95°C in a glass reactor. Small pieces of 3*3 mm cotton sheets (having a weight about 1-2 mg) were added to the reactor. The cellulose concentration, reaction time and temperature are the three variable parameters chosen to build the design of the experiment with a total of 14 different sets of parameters (Ex: T=60°C, t=16 h, c=2%). The treatment conditions to build the experimental domain in the design of experiments were chosen based on preliminary tests, conditions used in the literature and environmental aspects. For this reason, a lower range of temperatures than those reported in the literature and longer reaction times were tested.

At the end of the treatment, 200 ml of deionized water was added to the reactor to quench the reaction and reduce the viscosity of the mixture. The treated cellulose was washed and filtered through a membrane of 1 µm. The retained fibres were dispersed in water and filtered again, and this action was repeated 3 times. The filtrates were centrifuged at 10,000 rpm for 15 minutes with a small quantity of sodium chloride, and the cellulose nanocrystals obtained were dialysed until the conductivity of the sample was the same as that of deionized water.

2.3. Design of experiment and data analysis

The software MINITAB (MINITAB ®, LLC) was used for the statistical design of experiments and data analysis. To optimize the yield and crystallinity of the CNCs, three important treatment variables are chosen: treatment time (X_1), reaction temperature (X_2) and initial cellulose concentration (X_3). Their range and values are shown in Table 1.

Table 1: Reaction parameters and their values

Factor	Name	Range of actual and coded variables			
		Unit	-1	0	1
X_1	Reaction time	h	2	9	16
X_2	Temperature	°C	60	75.5	95
X_3	Concentration	%	1	1.5	2

Central composite design (CDD) is commonly used for improving and optimizing processes to fit a model by the least-squares technique. The method contains three steps: (i) design and experiments; (ii) response surface modelling through regression; and (iii) optimization of parameters.

Using the CCD model, the nanocrystal yield and crystallinity can be modelled by two functions (Y_y and Y_c, respectively) of the three parameters; the equation can be written as follows (Equation 1):

Equation 1

$$Y_y \text{ or } Y_c = b_0 + b_1X_1 + b_2X_2 + b_3X_3 + b_{12}X_1X_2 + b_{13}X_1X_3 + b_{23}X_2X_3 + b_{11}X_1X_1 + b_{22}X_2X_2 + b_{33}X_3X_3$$

The predicted response (Y_c or Y_y) is correlated to the set of regression coefficients: the intercept (b_0), the linear coefficients (b_1, b_2, b_3), the interaction coefficients (b_{12}, b_{13}, b_{23}) and the quadratic coefficients (b_{11}, b_{22}, b_{33}).
These different coefficients are calculated using the 14 treatment conditions determined by the CDD method; 3 treatment conditions in the domain centre are realized.

2.4. Nanocrystal and residual fibre analyses

CNC and residual fibre (RF) yield

As previously mentioned, residual fibres and cellulose nanocrystals were separated after acid treatment, which enabled the determination of the real CNC yield before the ultrasonic treatment.
The cellulose nanocrystal yield is calculated as the weight ratio of cellulose nanocrystals (m_CNC) and the initial weight of cellulose fibres (m_0), as expressed in Equation 2. At least two measurements were performed for each sample.

Equation 2

$$Y\_CNC\ (\%) = ((m\_CNC - m\_0\ ))/m\_0\ \ x\ 100$$

The residual fibre (RF) yield was also calculated using the same method (Equation 3).

Equation 3

$$Y\_RF\ (\%) = ((m\_RF - m\_0\ ))/m\_0\ \ x\ 100$$

Crystallinity Index by x-ray diffraction (XRD)

The crystallinity index (CI) of the cellulose nanocrystals was determined by the amorphous subtraction method. The area under the curve of an amorphous standard was subtracted from the sample area, and this difference was divided by the area of the sample as expressed in Equation 4. The measurements were realized in the dry CNC sample (overnight, 105°C) using an X'Pert Pro MDP instrument (Malvern Panalytical) in reflection mode with the Bragg Brentano geometry. The anode was composed of copper, and the wavelength was 1.5419 Angström. In this publication, the amorphous sample was bleached birch cellulose pulp cryo-crushed for twenty minutes using a Cryomill device (Retsch).

Equation 4

$$CI\%_{CNC} = (Area_{CNC} - Area_{amorphous})/Area_{CNC}\ \ x100$$

CNC sonicated suspension

A determined quantity of CNC was diluted to a concentration of 10^{-2} wt%. Using a 250-Watt sonication probe (Sonifer 250, Branson), the suspension was exposed to a dispersive energy of 8.7 MJ per gram of dried CNC at 50% of maximum energy.

Atomic force microscopy (AFM)

One drop of the sonicated CNC suspension was deposited on a mica plate and dried at room temperature overnight. Images were obtained using AFM (Dimension Icon) in tapping mode, and the mean height of individual nanocrystals was obtained using at least 50 measurements.

Transmission electronic microscopy (TEM)

A few drops of the CNC sonicated suspensions were deposited onto a glow-discharged carbon-coated copper grid. After 2 min, the excess liquid was removed with filter paper, and a droplet of 2 wt% uranyl acetate was deposited onto the grid before completely drying the CNCs. The excess stain was removed, and the specimens were observed with a JEOL JEM 2100-Plus microscope operating at 200 kV. A minimum of 10 digital images were recorded at different locations with a Gatan Rio 16 camera, and the most representative image was used for the discussion.

Fourier transform infrared spectrometry (FTIR)

Infrared spectra were obtained from cotton cellulose fibres and residual fibres using a Perkin-Elmer Spectrum 65 instrument (PerkinElmer, USA). The fibres were dried at room temperature overnight, and a KBr pellet was pressed from the powder containing 2% fibre. Spectra were recorded in transmission mode between 4000 and 400 cm^{-1} with 16 scans.

Residual fibre morphology

Residual fibre morphology analysis (length, width, number of elements, etc.) was carried out using the MorFi device (MorFi compact, Techpap). Images of a suspension of residual fibres at 40 g/L between the measurement cells were acquired to perform the image analysis. Elements whose length exceeded 100 µm were counted as fibres and those with a length below 100 µm were counted as fines. This measurement was performed in triplicate.

Scanning Electron Microscopy (SEM)

Scanning electron microscopy images were obtained with an ESEM instrument (Quanta 200, FEI, Japan) at an acceleration voltage of 10 kV. Wet samples of cotton fibres and residual fibres were air-dried and coated with carbon using a vacuum sputter coater. At least 20 images were taken, and the most representative images were used in the discussion.

3. Results and discussion

3.1. Model determination of the CNC yield.

The 17 conducted experiments are described in Table 2, and the obtained cellulose nanocrystal yields are reported in the penultimate column. The last column corresponds to the optimal normalization of the yield using the Cox-Box transformation method (λ=0.33) (Box and Cox, 1964).

Table 2: List of experimental parameters and obtained yields

Experiment Name	Concentration	Time	Temperature	CNC Yield	Cox-Box transformation
	%	h	°C	%	λ = 1/3
A	1.5	9	77.5	17.6	2.60
A’	1.5	9	77.5	22.8	2.83
A’’	1.5	9	77.5	18.4	2.64
B	1	2	60	0.3	0.65

C	2	16	60	4.9	1.70
D	2	2	95	18.3	2.63
E	1	16	60	10.2	2.17
F	1	2	95	30.7	3.13
G	2	2	60	0.7	0.88
H	2	16	95	24.5	2.90
I	1	16	95	21.7	2.79
J	1.5	9	60	1.7	1.20
K	1.5	16	77.5	5.0	3.09
L	1.5	9	95	29.7	2.95
M	2	9	77.5	25.6	1.95
N	1.5	2	77.5	7.4	1.71
O	1	9	77.5	14.5	2.44

Three replications were performed in the domain centre to assess the reproducibility of the treatment conditions (A, A' and A'').

The first response studied was the CNC yield. The coefficients of the models were determined according to the DOE results, and some insignificant interactions were detected and removed using the analysis of variance (ANOVA) method without degrading the model and maintaining a hierarchical structure. The final equation is expressed below (Equation 5), and the surface response of the CNC yield according to the temperature and the reaction time is plotted in Figure 1**Erreur ! Source du renvoi introuvable.**A, whereas the coefficient p-values and regression coefficient are shown in Figure 1B.

Equation 5

$$Y_y(\%) = (-3.758 + 0.397 \times t(h) + 0.068 \times T(°C) - 0.002 \times T(°C) \times t(h) - 0.010 \times t^2(h))^3$$

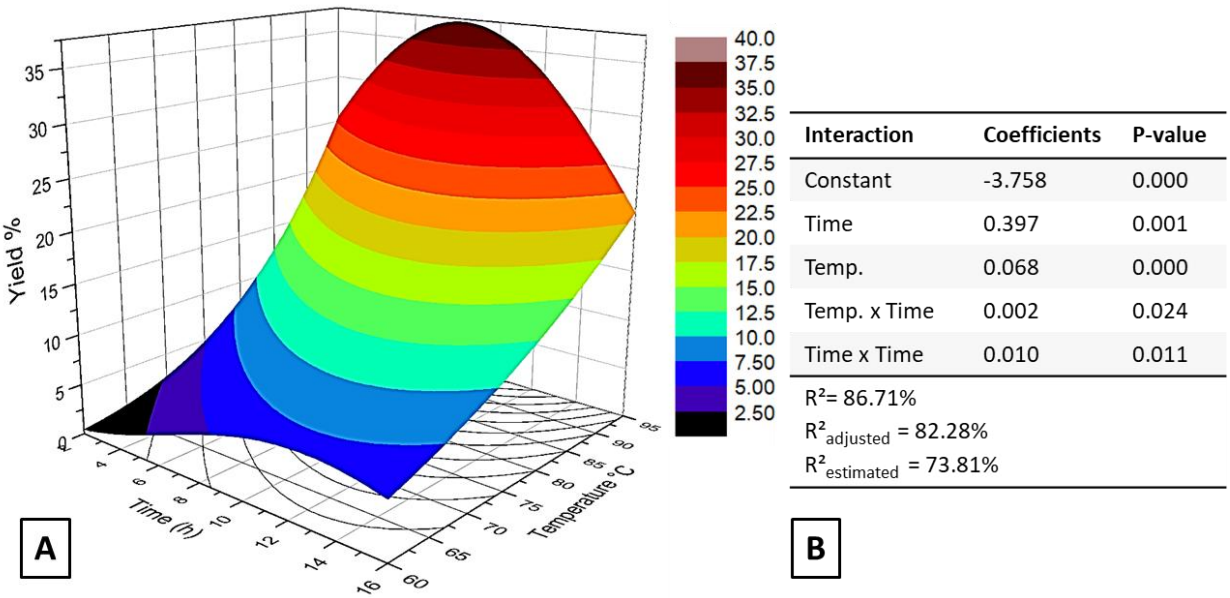

Interaction	Coefficients	P-value
Constant	-3.758	0.000
Time	0.397	0.001
Temp.	0.068	0.000
Temp. x Time	0.002	0.024
Time x Time	0.010	0.011

R^2= 86.71%
$R^2_{adjusted}$ = 82.28%
$R^2_{estimated}$ = 73.81%

Figure 1: A. Surface response of the yield - B. Regression coefficients and p-values of the coefficients

The fit of the model can be evaluated using the tree regression coefficients R-square (R^2), adjusted R-square ($R^2_{adjusted}$), and estimated R-square ($R^2_{estimated}$); the closer their values are to 100%, the better the model fits. In the current model, R^2 and $R^2_{adjusted}$ were higher than 80%, and the difference between $R^2_{adjusted}$ and $R^2_{estimated}$ was lower than 10%; as a consequence, the model can be used with caution.

The first observation of this model is that the fibre concentration during the treatment did not influence the final yield; indeed, all the mathematical terms of the model, including the concentration, were negligible. The initial concentration range of cellulosic cotton fibres (1-2%) was determined using preliminary experiments to obtain a good dispersion of the fibres in the NADES while limiting the viscosity of the reaction medium. Indeed, ChCl:OAD 1:1 is a viscous solvent, especially at low temperature, and adding cellulose fibres further increases the global viscosity of the mixture. The starting hypothesis consisted of the fact that increasing the fibre concentration would reduce the efficiency of the treatment due to the limited penetration of the chemicals into the cotton fibres. In practice, the small variation in the concentration in the experimental domain did not allow us to observe the influence of this parameter on the yield optimization because the viscosity of the mixture was likely the same. This result also confirmed the large excess of acid, which facilitated the hydrolysis of the amorphous part in the experimental domain.
As expected, the temperature played a crucial role in the extraction of the cellulose nanocrystal. The higher the treatment temperature , the higher the final CNC yield. This trend had already been observed by Sirviö in 2016 (Sirviö, Visanko, and Liimatainen, 2016), but another study by Liu *et al*. showed that microwave application reduced the CNC yield a high temperatures (Liu *et al*., 2017). These results are not truly in contradiction because the cellulosic fibre sources, as well as the experimental conditions used, were different in the three studies (Table 3). Moreover, in all cases, the yield in this approach increased with temperature and started to decrease when the degradation took place.

The treatment time is also a very important parameter, and as observed in the surface response (Figure 1), the CNC yield decreased after 8 or 9 hours of treatment. Moreover, the residual fibres were brownish after this time, and after 16 h of treatment, even the CNC nanoparticles became partially coloured, as already observed by Liu *et al*., who reported the same tendency. Both phenomena may be due to the degradation of the cellulose material because of the strong condition of treatment.

Since the theoretical mathematical model was defined, we proceeded with the next step aiming at its validation by performing a new experiment within the domain. The chosen parameters for this experiment targeted a theoretical maximum CNC yield of 37.2 ± 2.7%, which theoretically could be obtained after 8 hours and 13 minutes of treatment at 95°C.

In this context, these optimal experimental conditions were tested in triplicate with a chosen fibre concentration of 1%.
This set of parameters resulted in a CNC yield of approximately 44.9 ± 2.5%. The difference between the theoretical and experimental values was higher than expected but still acceptable. In fact, even if a few points of higher yield were

observed, the standard deviation was a perfect fit with the theoretical value. Some hypotheses can be drawn to explain this slight discrepancy. The optimum point is located close to the maximum of the theoretical curve (maximum temperature T=95°C), whereas the mathematical model obtains a better fit in the centre. It is possible that some unknown parameters governing the studied reaction were neglected when building the model. Finally, the polynomial law is not perfectly suitable to properly describe the reaction.

The cellulose nanocrystals (obtained using the treatment conditions ChCl:OAD, 95°C, 8 h 13 min, c=1%) were characterized and can be compared to those of CNC obtained in the literature using deep eutectic solvents composed of choline chloride and oxalic acid dihydrate (Table 3).

Table 3: Overview of the different pre-treatment conditions using ChCl:OAD NADES for obtaining cellulose nanocrystals - adapted from Le Gars *et al.,* 2019

Cellulose source	**Treatment (DES, …)**	**Molar Ratio**	**Time**	**Temp. °C**	**Yield* %**	**Dimension nm**	**Ref**
Dissolving pulp	ChCl : OAD	1:1	2 h	100	68	l = 390 ± 25 d = 13.6 ± 1.1	Sirviö, Visanko, and Liimatainen 2016
		1:1	2 h	120	73	l = 353 ± 16 d = 13.8 ± 0.7	
Dissolving pulp	ChCl : OAD	1:1	30 min	100	NA	l = 50 - 350 d = 3-8	Laitinen *et al.* 2017
Cotton fibre	ChCl : OAD	1:1	1 h	100	79.8	l = 194.1 d = 9.6 ± 2.9	Ling *et al.* 2019
	ChCl : OAD	1:2	1 h	100	80.0	l = 152.7 d = 6.1 ± 1.2	
	ChCl : OAD	1:3	1 h	100	81.6	l = 122.4 d = 4.7 ± 2.2	
Cotton fibre	ChCl : OAD *Microwave assisted*	1:1 *800W*	3 min	80	74.2	l = 100-350 d = 3-25	Liu *et al.* 2017
		1:1 *800W*	3 min	90	62.4	NA	
		1:1 *800W*	3 min	100	57.8	l ≈ 150 d < 17	
Bleached eucalyptus kraft pulp	ChCl : OAD *+ catalyst: FeCl3 . 6H2O (mmol/gDES)*	1:4 *0*	7 h	80	86	l = 5152 ± 3328	Yang *et al.* 2019
		1:4 *0.15*	6 h	80	73	l = 270 ± 92	
		1:4 *0.3*	6 h	80	71	l = 258 ± 54	
		1:1 *0.15*	6 h	80	88	l = 5726 ± 3856	
Bleached cotton fibre: 14 exp.	ChCl : OAD	1:1	2-16 h	60-95	0.3-30.7	NA	This study
Bleached cotton fibre: yield optimization		1:1	8 h 13	95	CNC= 44.9% Fibre= 13.6%	l= 282 ± 46 d= 7.9 ± 1.9	

*Yield means yield of CNC and residual fibres except in our study
NA: non-applicable

The CNC morphology was determined after sonication of the suspensions, and their height was deduced from AFM images, whereas their length was deduced from TEM images. Fifty measurements of individual CNC were conducted, and the mean height value was 7.9 ± 1.9 nm, while their length was approximately 282 ± 46 nm. These values are similar to those associated with the CNC dimensions obtained from cotton *via* classical acid hydrolysis (Dufresne, 2017) and those obtained by ChCl:OAD treatment (Liu *et al*., 2017; Ling *et al*., 2019). TEM and AFM images of our cellulose nanocrystals are displayed in Figure 2.

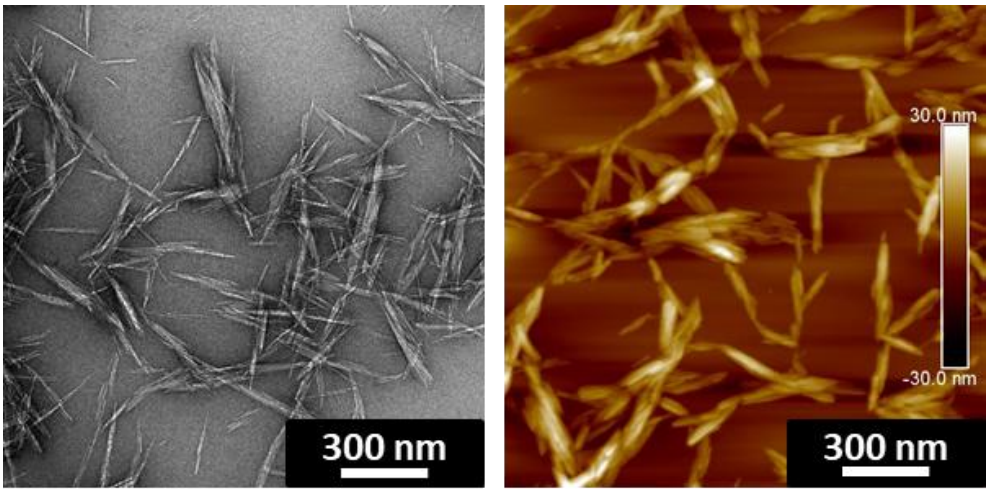

Figure 2: Cellulose nanocrystals after treatment with ChCl:OAD (1:1), 95°C, 8 h 13 min: - Left. TEM image - Right. AFM image

The obtained CNC yield was lower than the yield found in the literature. This difference can be attributed to the washing and separation steps after NADES treatment, which were different from those reported in the publications cited in Table 3. Indeed, in this work, residual fibres and CNC were separated before the ultrasonic treatment step and two distinguished suspension were obtained. The consequences are that some cellulose nanocrystals were removed along with the residual cellulose fibres and/or with the large CNC aggregates that were filtered out by the filtration membrane.

Using these "optimal" conditions, a small quantity of residual fibres was obtained (yield of fibres: 16.3%), and their morphology was compared with the initial dimension of cotton fibres (see Table 4). After the ChCl:OAD 1:1 treatment, the residual fibres exhibited a mean length divided by five and a number of fines multiplied by thirty-eight compared to the initial values, which confirmed the fragmentation capacity of NADES. Scanning electron microscopy images of fibres before and after treatment are shown in the supporting information (Figure S 1).

Table 4: Morphology of residual fibres.

	Fibres		**Fines**	
	Mean length µm	**Mean width µm**	**Fines content millions/g**	**Mean length µm**
Reference Cotton Fibres	689 ± 10	25 ± 0	67 ± 3	49 ± 0
Residual Fibres	131 ± 1	21 ± 1	2531 ± 197	23 ± 1

The cotton fibre and the residual fibre morphology result from the optical analysis of the respective suspensions by the MorFi device. This device divides the counted elements into subcategories. Figure 3 shows an example of the measurement reproducibility obtained by comparing the mean length of fines contained in the residual fibre suspension for the three previous treatment conditions (8 h 13 min, 95°C). According to the morphology analysis of the initial fibers, as expected, there is a big distribution of the fibres' size. As a consequence, big fibres or agglomerates would take much more time to be reduced to nanosize. This is the reason one, at the end of the reaction, some residual fibres are still present. Indeed, the quantity of this residue decrease with increasing reaction time.

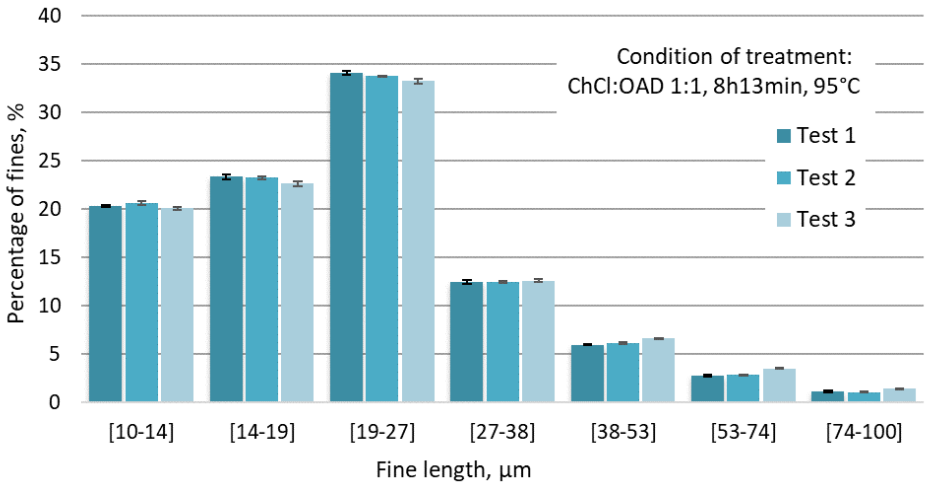

Figure 3: Fine mean length contained in the residual fibre suspension (measured in triplicate with ChCl:OAD 1:1, 8 h 13 min, 95°C treatment conditions)

The infrared spectrum was obtained from the residual fibres and compared to that of the cotton fibres, and no new absorption peak was observed in the residual fibre spectrum. This result demonstrates that no chemical reaction took place on the cellulose (supporting information Figure S 2).

3.2. Model determination for the crystallinity

To determine the theoretical equation of the cellulose nanocrystal crystallinity, the same methodology as that for the CNC yield was used. The crystallinity index (CI) of the cellulose nanocrystals previously obtained from the 17 experiments were evaluated by the amorphous subtraction method and are reported in Table 5.

Table 5: List of experimental parameters and the obtained crystallinity

Experiment Name	Concentration	Time	Temperature	CNC CI
	%	H	°C	%
Ref	-	-	-	79
A	1.5	9	77.5	79
A'	1.5	9	77.5	79
A''	1.5	9	77.5	77
B	1	2	60	61
C	2	16	60	73
D	2	2	95	78

E	1	16	60	71
F	1	2	95	78
G	2	2	60	65
H	2	16	95	80
I	1	16	95	80
J	1.5	9	60	66
K	1.5	16	77.5	80
L	1.5	9	95	81
M	2	9	77.5	80
N	1.5	2	77.5	72
O	1	9	77.5	78

The amorphous subtraction method with cellulosic samples has been described in the literature (Isogai and Usuda, 1989), and over the last decade, it has been compared to other methods (Park *et al*., 2010; Ahvenainen, Kontro, and Svedström, 2016). The main challenge of this method is choosing a good amorphous sample that fits the sample under investigation. In this publication, the chosen amorphous sample was bleached, cryo-crushed birch cellulose pulp.

As previously mentioned, three repetitions were performed in the domain centre to assess the reproducibility of the treatment conditions (A, A' and A''). This time, Box-Cox transformation was not required to analyse the data, and the obtained theoretical model is described by Equation 6.

Equation 6

$$Y_{crystallinity}(\%) = -50.9 + 2.769 \times T(°C) + 2.188 \times t(h) - 6.46 \times c(\%) - 0.01396 \times T^2(°C) - 0.0362 \times t^2(h) + 4.90 \times c^2(\%) - 0.01429 \times T(°C) \times t(h) - 0.0857 \times T(°C) \times c(\%)$$

In contrast to the CNC yield, the CNC crystallinity depended on the initial concentration of the cellulosic fibres. The surface response of the CNC crystallinity according to the temperature and the reaction time for a fixed concentration value of 2 wt% is plotted in Figure 4A, and the coefficient p-values and regression coefficient are shown in Figure 4B.

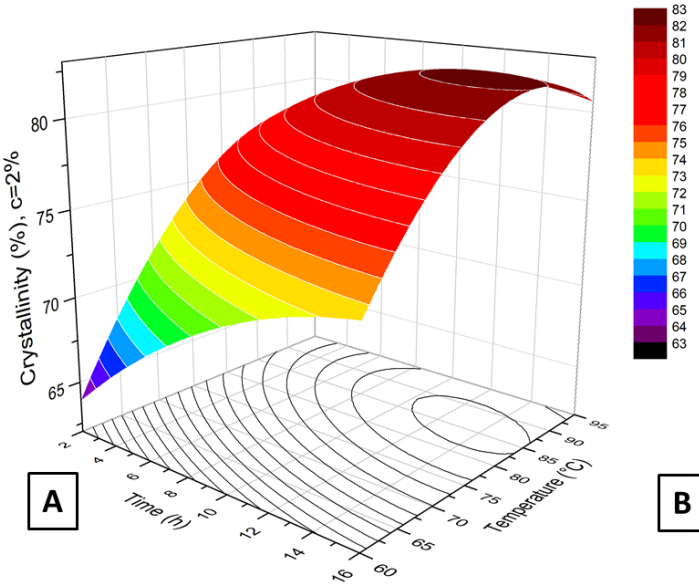

Interaction	Coefficients	P-value
Constant	-50.9	0.000
Temperature	2.769	0.000
Time	2.188	0.000
Concentration	-6.46	0.071
Temp. x Time	-0.01429	0.004
Temp. x concent.	-0.0857	0.119
Temp. x Temp.	-0.01396	0.000
Time x Time	-0.0362	0.044
Concent. x concent.	4.9	0.138

B

R^2= 98.04%
$R^2_{adjusted}$ = 96.08%
$R^2_{estimated}$ = 90.96%

Figure 4: A. Surface response of the crystallinity (c= 2%) - B. Regression coefficients and p-values of the coefficients.

The regression coefficients of this model were R^2= 98.0% and $R^2_{estimated}$ = 91.0%, and thus, the mathematical model can be used with the recommendation to test a new point in the domain when designing the experimental strategy. The crystallinity of the CNC obtained with the conditions for the yield optimization (T= 95°C, t= 8 h 13 min, c= 1%) was evaluated for the three repetitions. The theoretical value expected for these parameters was CI%= 81 ± 1%, and the mean experimental value was 82 ± 1%. In conclusion, the model was able to predict the crystallinity of the obtained CNCs in all experimental domains. The cellulose nanocrystal crystallinity seemed to reach a maximum after approximately 13 h of treatment at 85°C using an initial concentration of 2%. These crystallinity values were high but similar to those reported by Ling *et al.* (Ling *et al.*, 2019). They obtained dispersed CNCs with a crystallinity index of 75% using cotton fibres treated with ChCl:OAD 1:1 for 1 h at 80°C, and the theoretical model found in this study predicted a CI of 75% for the CNC product treated at 80°C for 2 hours. It is worth mentioning the rather excellent agreement between theoretical and experimental data in this section. Thus, it can be concluded that: For low temperature experiments the crystallinity index decreased most probably because of the formation of amorphous zones due to the swelling of the fibres and before starting the hydrolysis step. Instead, for high temperature experiment did not affect significantly the CI(%) because the swelling and the hydrolysis took place simultaneously. In all cases, the changes on this parameter are hard to ascertain because of the relatively high crystallinity of the starting materials (CI(%) = 79%).

3.3. Response's combination

The strength of the design of the experimental method is the possibility of the response's combination. Reporting the two models previously described for the CNC yield (%) and the crystallinity index (%) in a two-dimensional graph simplifies the choice of the parameters that can optimize the two responses simultaneously (Figure 5). The main objective of this graph is its capacity to predict CNC concentration and crystallinity for a given set of parameters.

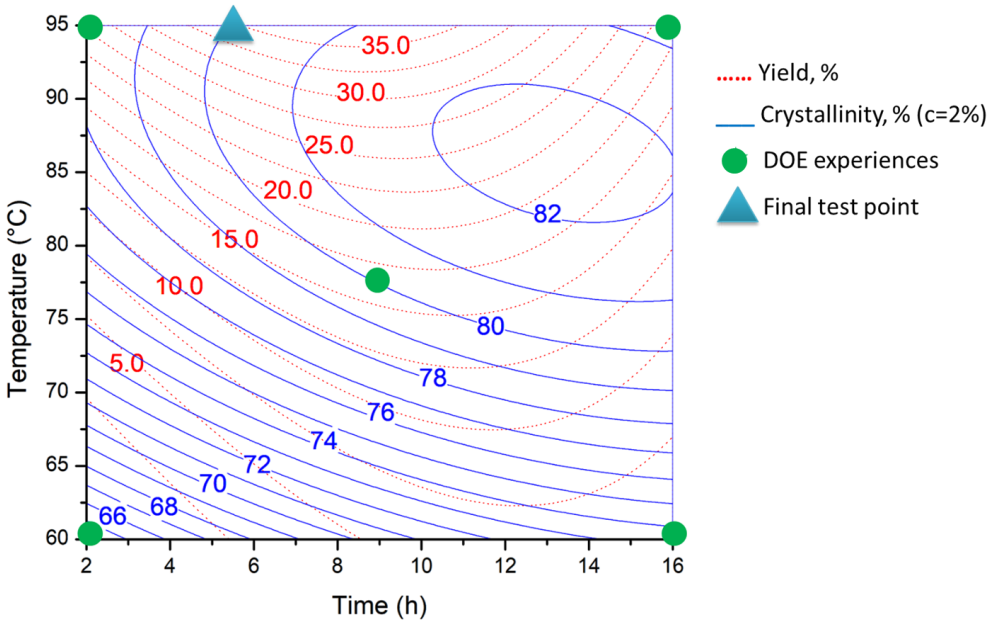

Figure 5: Overlay of the contour diagrams for the two studied responses: Yield% and Crystallinity% (c=2%).

The actual aim was the production of cellulose nanocrystals in large quantities and, if possible, at high concentrations. Therefore, the CNC yield was more relevant than the crystallinity. Moreover, a short reaction time was recommended. Indeed, the available CNC production processes using classical acid hydrolysis are carried out in less than 1 hour. Furthermore, between 6 and 8 hours of treatment at 95°C, the gain in CNC yield and crystallinity was very low. Considering this information, a new set of parameters was chosen to carry out a final experiment: a reaction time of 6 hours at a temperature of 95°C and an initial concentration of cotton cellulosic fibres of 2% (bleu triangle in Figure 5).

For these parameters, the expected CNC yield was approximately 35.5 ± 2.7% with a crystallinity index of 80 ± 1%. Three experiments were carried out for reproducibility, and the results were a CNC yield of 43.6 ± 1.9% and a crystallinity of 81 ± 1%. Similar to the previous experiments, the obtained CNC yield was higher than expected and was relatively close to the yield obtained after 8 h 13 mins of treatment (44.9 ± 2.5%). The mathematical model for CNC crystallinity was again confirmed. The CNC morphology was determined after sonication of the suspensions, and their height was obtained from AFM images, whereas their length was obtained from TEM images. Fifty measurements of individual CNCs were conducted, and the mean height value was found to be 11.3 ± 2.6 nm, while their length was approximately 257 ± 54 nm. TEM and AFM images of these cellulose nanocrystals are shown in Figure 6.

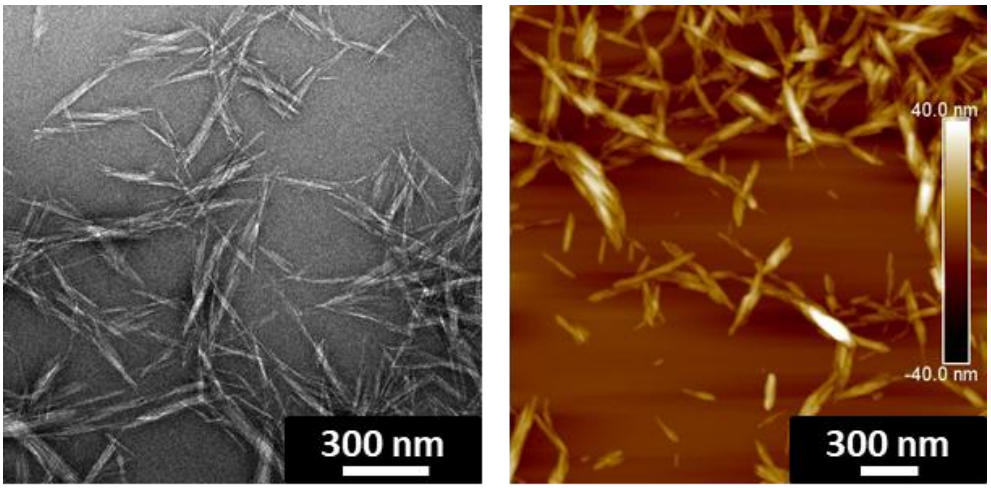

Figure 6: TEM (left) and AFM (right) images of CNCs obtained after 6 h of treatment at 95°C with a fibre concentration of 2%.

4. Conclusion

In this work, cellulose nanocrystals were successfully extracted using an acidic NADES composed of choline chloride:oxalic acid dihydrate at a molar ratio of 1:1. To optimize the treatment time and temperature in the acidic hydrolysis of the amorphous regions of cellulose, the methodology of the design of the experiment was used. Two models were established to characterize the evolution of the nanoparticle's crystallinity and the CNC yield of the treatment. Our hypothesis has been confirmed and optima yield and CNC crystallinity have been found thanks to the design of experiment approach. The first model successfully described the crystallinity variation of CNCs according to the different treatment parameters, while the second model was less accurate for describing the experimental values and provided slightly higher values, although it followed the same tendency. The obtained results are highly useful because, to the best of our knowledge, this is the first time that this optimization work has been proposed. This study shows that it is possible to predict the CNC yield CNC and their crystallinity thanks to predictive mathematical models, which gives a great advantage to consider in the near future a scale up of the extraction of cellulose nanocrystals using this original family of green solvents.
The next step should be an evaluation of different cellulose sources and NADES compositions by DOE to validate whether the methodology can be applied to any type of CNC extraction by an acidic NADES.

Acknowledgements

This research was made possible thanks to the facilities of the TekLiCell platform funded by the Région Rhône-Alpes (ERDF: European regional development fund).
The authors acknowledge Cecile Sillard (LGP2, Grenoble) for AFM images, Christine Lancelon-Pin (CERMAV, Grenoble) for TEM images, and Gabriel Banvillet (LGP2, Grenoble) for the cellulose amorphous reference used in the crystallinity study.

References

544 Abbott, Andrew P., Glen Capper, David L. Davies, Raymond K. Rasheed, and Vasuki
545 Tambyrajah. 2003. 'Novel Solvent Properties of Choline Chloride/Urea
546 MixturesElectronic Supplementary Information (ESI) Available: Spectroscopic Data. See
547 Http://Www.Rsc.Org/Suppdata/Cc/B2/B210714g/'. *Chemical Communications*, no. 1
548 (December): 70–71. https://doi.org/10.1039/b210714g.
549 Ahvenainen, Patrik, Inkeri Kontro, and Kirsi Svedström. 2016. 'Comparison of Sample
550 Crystallinity Determination Methods by X-Ray Diffraction for Challenging Cellulose I
551 Materials'. *Cellulose* 23 (2): 1073–86. https://doi.org/10.1007/s10570-016-0881-6.
552 Araki, Jun, Masahisa Wada, Shigenori Kuga, and Takeshi Okano. 1999. 'Influence of Surface
553 Charge on Viscosity Behavior of Cellulose Microcrystal Suspension'. *Journal of Wood Science*
554 45 (3): 258–61. https://doi.org/10.1007/BF01177736.
555 Box, G. E. P., and D. R. Cox. 1964. 'An Analysis of Transformations'. *Journal of the Royal Statistical*
556 *Society. Series B (Methodological)* 26 (2): 211–52.
557 Bras, Julien, David Viet, Cécile Bruzzese, and Alain Dufresne. 2011. 'Correlation between
558 Stiffness of Sheets Prepared from Cellulose Whiskers and Nanoparticles Dimensions'.
559 *Carbohydrate Polymers* 84 (1): 211–15. https://doi.org/10.1016/j.carbpol.2010.11.022.
560 Domingues, Rui M. A., Manuela E. Gomes, and Rui L. Reis. 2014. 'The Potential of Cellulose
561 Nanocrystals in Tissue Engineering Strategies'. *Biomacromolecules* 15 (7): 2327–46.
562 https://doi.org/10.1021/bm500524s.
563 Du, Haishun, Wei Liu, Miaomiao Zhang, Chuanling Si, Xinyu Zhang, and Bin Li. 2019. 'Cellulose
564 Nanocrystals and Cellulose Nanofibrils Based Hydrogels for Biomedical Applications'.
565 *Carbohydrate Polymers* 209 (April): 130–44. https://doi.org/10.1016/j.carbpol.2019.01.020.
566 Dufresne, Alain. 2017. *Nanocellulose: From Nature to High Performance Tailored Materials*. Walter de
567 Gruyter GmbH & Co KG.
568 Filson, P, and B Dawsonandoh. 2009. 'Sono-Chemical Preparation of Cellulose Nanocrystals
569 from Lignocellulose Derived Materials'. *Bioresource Technology* 100 (7): 2259–64.
570 https://doi.org/10.1016/j.biortech.2008.09.062.
571 Flauzino Neto, Wilson Pires, Hudson Alves Silvério, Noélio Oliveira Dantas, and Daniel
572 Pasquini. 2013. 'Extraction and Characterization of Cellulose Nanocrystals from Agro-
573 Industrial Residue – Soy Hulls'. *Industrial Crops and Products* 42 (March): 480–88.
574 https://doi.org/10.1016/j.indcrop.2012.06.041.
575 Francisco, María, Adriaan van den Bruinhorst, and Maaike C. Kroon. 2013. 'Low-Transition-
576 Temperature Mixtures (LTTMs): A New Generation of Designer Solvents'. *Angewandte*
577 *Chemie International Edition* 52 (11): 3074–85. https://doi.org/10.1002/anie.201207548.
578 Gicquel, Erwan, Julien Bras, Candice Rey, Jean-Luc Putaux, Frédéric Pignon, Bruno Jean, and
579 Céline Martin. 2019. 'Impact of Sonication on the Rheological and Colloidal Properties of
580 Highly Concentrated Cellulose Nanocrystal Suspensions'. *Cellulose* 26 (13–14): 7619–34.
581 https://doi.org/10.1007/s10570-019-02622-7.
582 Haldar, Dibyajyoti, and Mihir Kumar Purkait. 2020. 'Micro and Nanocrystalline Cellulose
583 Derivatives of Lignocellulosic Biomass: A Review on Synthesis, Applications and
584 Advancements'. *Carbohydrate Polymers* 250 (December): 116937.
585 https://doi.org/10.1016/j.carbpol.2020.116937.
586 Ibrahim, A, M F Abdullah, and S T Sam. 2018. 'Hydrolysis Empty Fruit Bunch (EFB) Using
587 Green Solvent'. *IOP Conference Series: Materials Science and Engineering* 429 (November):
588 012059. https://doi.org/10.1088/1757-899X/429/1/012059.
589 Isogai, Akira. 2020. 'Emerging Nanocellulose Technologies: Recent Developments'. *Advanced*
590 *Materials* n/a (n/a): 2000630. https://doi.org/10.1002/adma.202000630.
591 Isogai, Akira, and Makoto Usuda. 1989. 'Crystallinity Indexes of Cellulosic Materials'. *Sen'i*
592 *Gakkaish*, no. 46: 324–329.
593 Laitinen, Ossi, Jonna Ojala, Juho Antti Sirviö, and Henrikki Liimatainen. 2017. 'Sustainable
594 Stabilization of Oil in Water Emulsions by Cellulose Nanocrystals Synthesized from

595 Deep Eutectic Solvents'. *Cellulose* 24 (4): 1679–89. https://doi.org/10.1007/s10570-017-
596 1226-9.
597 Le Gars, Manon, Loreleï Douard, Naceur Belgacem, and Julien Bras. 2019. 'Cellulose
598 Nanocrystals: From Classical Hydrolysis to the Use of Deep Eutectic Solvents'. In
599 *Nanosystems [Working Title]*. IntechOpen. https://doi.org/10.5772/intechopen.89878.
600 Li, Panpan, Juho Antti Sirviö, Bright Asante, and Henrikki Liimatainen. 2018. 'Recyclable Deep
601 Eutectic Solvent for the Production of Cationic Nanocelluloses'. *Carbohydrate Polymers* 199
602 (November): 219–27. https://doi.org/10.1016/j.carbpol.2018.07.024.
603 Ling, Zhe, J. Vincent Edwards, Zongwei Guo, Nicolette T. Prevost, Sunghyun Nam, Qinglin
604 Wu, Alfred D. French, and Feng Xu. 2019. 'Structural Variations of Cotton Cellulose
605 Nanocrystals from Deep Eutectic Solvent Treatment: Micro and Nano Scale'. *Cellulose* 26
606 (2): 861–76. https://doi.org/10.1007/s10570-018-2092-9.
607 Liu, Yongzhuang, Bingtuo Guo, Qinqin Xia, Juan Meng, Wenshuai Chen, Shouxin Liu, Qingwen
608 Wang, Yixing Liu, Jian Li, and Haipeng Yu. 2017. 'Efficient Cleavage of Strong Hydrogen
609 Bonds in Cotton by Deep Eutectic Solvents and Facile Fabrication of Cellulose
610 Nanocrystals in High Yields'. *ACS Sustainable Chemistry & Engineering* 5 (9): 7623–31.
611 https://doi.org/10.1021/acssuschemeng.7b00954.
612 Man, Zakaria, Nawshad Muhammad, Ariyanti Sarwono, Mohamad Azmi Bustam, M. Vignesh
613 Kumar, and Sikander Rafiq. 2011. 'Preparation of Cellulose Nanocrystals Using an Ionic
614 Liquid'. *Journal of Polymers and the Environment* 19 (3): 726–31.
615 https://doi.org/10.1007/s10924-011-0323-3.
616 Mariano, Marcos, Nadia El Kissi, and Alain Dufresne. 2014. 'Cellulose Nanocrystals and Related
617 Nanocomposites: Review of Some Properties and Challenges'. *Journal of Polymer Science*
618 *Part B: Polymer Physics* 52 (12): 791–806. https://doi.org/10.1002/polb.23490.
619 Mascheroni, Erika, Riccardo Rampazzo, Marco Aldo Ortenzi, Giulio Piva, Simone Bonetti, and
620 Luciano Piergiovanni. 2016. 'Comparison of Cellulose Nanocrystals Obtained by Sulfuric
621 Acid Hydrolysis and Ammonium Persulfate, to Be Used as Coating on Flexible Food-
622 Packaging Materials'. *Cellulose* 23 (1): 779–93. https://doi.org/10.1007/s10570-015-0853-
623 2.
624 Nickerson, R. F., and J. A. Habrle. 1947. 'Cellulose Intercrystalline Structure'. *Industrial &*
625 *Engineering Chemistry* 39 (11): 1507–12. https://doi.org/10.1021/ie50455a024.
626 Novo, Lísias P., Julien Bras, Araceli García, Naceur Belgacem, and Antonio A. S. Curvelo. 2015.
627 'Subcritical Water: A Method for Green Production of Cellulose Nanocrystals'. *ACS*
628 *Sustainable Chemistry & Engineering* 3 (11): 2839–46.
629 https://doi.org/10.1021/acssuschemeng.5b00762.
630 Paiva, Alexandre, Rita Craveiro, Ivo Aroso, Marta Martins, Rui L. Reis, and Ana Rita C. Duarte.
631 2014. 'Natural Deep Eutectic Solvents – Solvents for the 21st Century'. *ACS Sustainable*
632 *Chemistry & Engineering* 2 (5): 1063–71. https://doi.org/10.1021/sc500096j.
633 Park, Sunkyu, John O Baker, Michael E Himmel, Philip A Parilla, and David K Johnson. 2010.
634 'Cellulose Crystallinity Index: Measurement Techniques and Their Impact on Interpreting
635 Cellulase Performance'. *Biotechnology for Biofuels* 3 (1): 10. https://doi.org/10.1186/1754-
636 6834-3-10.
637 Ramires, Elaine C., and Alain Dufresne. 2011. 'A Review of Cellulose Nanocrystals and
638 Nanocomposites'. *TAPPI Journal* 10 (4): 9–16. https://doi.org/10.32964/TJ10.4.9.
639 Reid, Michael S., Marco Villalobos, and Emily D. Cranston. 2017. 'Benchmarking Cellulose
640 Nanocrystals: From the Laboratory to Industrial Production'. *Langmuir* 33 (7): 1583–98.
641 https://doi.org/10.1021/acs.langmuir.6b03765.
642 Shankaran, Dhesingh Ravi. 2018. 'Chapter 14 - Cellulose Nanocrystals for Health Care
643 Applications'. In *Applications of Nanomaterials*, edited by Sneha Mohan Bhagyaraj,
644 Oluwatobi Samuel Oluwafemi, Nandakumar Kalarikkal, and Sabu Thomas, 415–59.

645 Micro and Nano Technologies. Woodhead Publishing. https://doi.org/10.1016/B978-0-
646 08-101971-9.00015-6.
647 Sirviö, Juho Antti. 2019. 'Fabrication of Regenerated Cellulose Nanoparticles by Mechanical
648 Disintegration of Cellulose after Dissolution and Regeneration from a Deep Eutectic
649 Solvent'. *Journal of Materials Chemistry A* 7 (2): 755–63.
650 https://doi.org/10.1039/C8TA09959F.
651 Sirviö, Juho Antti, Miikka Visanko, and Henrikki Liimatainen. 2016. 'Acidic Deep Eutectic
652 Solvents As Hydrolytic Media for Cellulose Nanocrystal Production'. *Biomacromolecules* 17
653 (9): 3025–32. https://doi.org/10.1021/acs.biomac.6b00910.
654 Smith, Emma L., Andrew P. Abbott, and Karl S. Ryder. 2014. 'Deep Eutectic Solvents (DESs)
655 and Their Applications'. *Chemical Reviews* 114 (21): 11060–82.
656 https://doi.org/10.1021/cr300162p.
657 Vanda, Henni, Yuntao Dai, Erica G. Wilson, Robert Verpoorte, and Young Hae Choi. 2018.
658 'Green Solvents from Ionic Liquids and Deep Eutectic Solvents to Natural Deep
659 Eutectic Solvents'. *Comptes Rendus Chimie* 21 (6): 628–38.
660 https://doi.org/10.1016/j.crci.2018.04.002.
661 Yang, Xianghao, Hongxiang Xie, Haishun Du, Xinyu Zhang, Zhufan Zou, Yang Zou, Wei Liu,
662 Hongyan Lan, Xinxing Zhang, and Chuanling Si. 2019. 'Facile Extraction of Thermally
663 Stable and Dispersible Cellulose Nanocrystals with High Yield via a Green and Recyclable
664 $FeCl_3$ -Catalyzed Deep Eutectic Solvent System'. *ACS Sustainable Chemistry & Engineering*
665 7 (7): 7200–7208. https://doi.org/10.1021/acssuschemeng.9b00209.
666 Zdanowicz, Magdalena, Katarzyna Wilpiszewska, and Tadeusz Spychaj. 2018. 'Deep Eutectic
667 Solvents for Polysaccharides Processing. A Review'. *Carbohydrate Polymers* 200
668 (November): 361–80. https://doi.org/10.1016/j.carbpol.2018.07.078.
669
670
671

Supporting information

Use of a natural acidic deep eutectic solvent to obtain a high yield and crystallinity of cellulose nanocrystals using the design of experience approach.

Douard L.[1], Bras J.[1,2], Encinas T.[3], Belgacem N.[1,4*]

1. Univ. Grenoble Alpes, CNRS, Grenoble INP, LGP2, F-38000 Grenoble, France
2. Nestle Research Center, CH-1000 Lausanne, Switzerland
3. Univ. Grenoble Alpes, CNRS, Grenoble INP, CMTC, F-38000 Grenoble, France
4. Institut Universitaire de France (IUF), F-75000 Paris, France

*Contact: mohamed-naceur.belgacem@grenoble-inp.fr

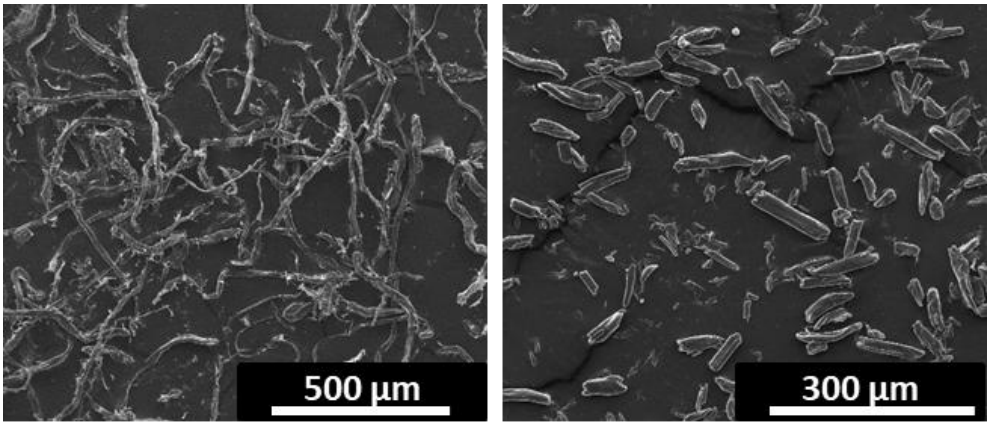

Figure S 1: SEM images of reference cotton fibres (left) and residual fibres after 8 h 13 min of treatment at 95°C (right)

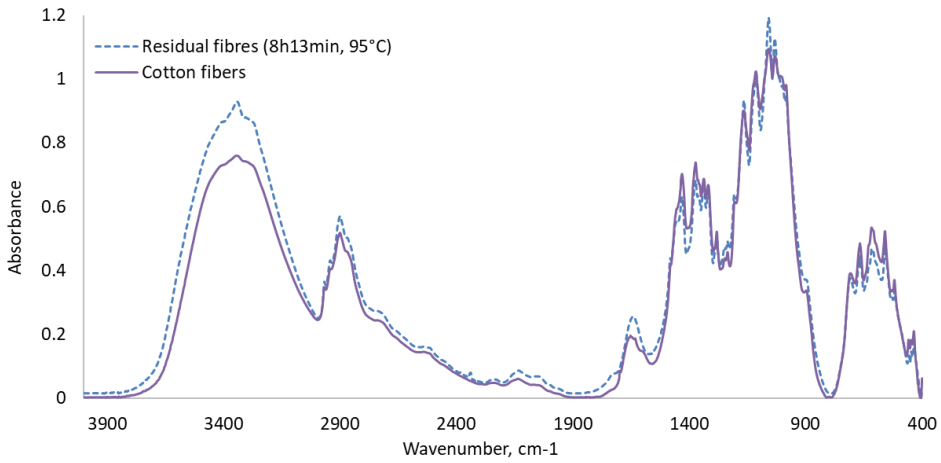

Figure S 2: Infrared spectra of cotton cellulosic fibres and residual fibres after 8 h 13 min of treatment at 95°C